

Bounds of redundant multicast routing problem with SRLG-diverse constraints: edge, path and tree models

Zhe Liang · Wanpracha Art Chaovalitwongse

Received: 16 June 2009 / Accepted: 11 November 2009 / Published online: 6 December 2009
© Springer Science+Business Media, LLC. 2009

Abstract This paper proposes three classes of alternative mathematical programming models (i.e., edge-based, path-based, and tree-based) for redundant multicast routing problem with shared risk link group (SRLG)-diverse constraints (RMR-SRLGD). The goal of RMR-SRLGD problem is to find two redundant multicast trees, each from one of the two sources to every destination, at a minimum cost while ensuring the paths from the two sources to a destination do not share any common risks. Such risk could cause the failures of multiple links simultaneously. Therefore, the RMR-SRLGD problem ensures the availability and reliability of multicast services. We investigated and compared the theoretical bounds of the linear programming (LP) relaxation for all models. We also summarized a hierarchy relationship of the tightness of LP bounds for the proposed models.

Keywords Mixed integer program · Multicast · Shared risk link groups

1 Introduction

In this paper, we study a redundant multicast routing problem on a directed network $G = (V, E)$, where V is a set of nodes and E is a set of edges (links). There are a set of two sources denoted by $S \subset V$ and a set of destinations denoted by $D \subset V$. There is a set of *shared risk link groups* (SRLGs) denoted by B . Each $b \in B$ contains a set of edges $E_b \subset E$, which are subject to a common risk. Each edge $(i, j) \in E$ in the network has an associated cost c_{ij} and belongs to one or more SRLGs. The objective of the problem is to find two multicast trees, one from each source $s \in S$ to all the destinations D with a minimum total cost, and ensures

Z. Liang · W. Art Chaovalitwongse (✉)
Department of Industrial & Systems Engineering, Rutgers University, 96 Frelinghuysen Road CoRE
Building, Room 201, Piscataway, NJ 08854, USA
e-mail: wchaoval@rci.rutgers.edu

Z. Liang
e-mail: zheliang@rci.rutgers.edu

any pair of paths from two sources to any destination are SRLG-diverse. We shall call the problem as RMR-SRLGD.

RMR-SRLGD arises in many network applications such as communication systems, power supply distribution systems, transportation network, etc. In these applications, there are common needs to transmit or deliver specific information or objects from a single source to a set of destinations [1,7,8], called *multicast group*. The edges used in multicast transmission form a multicast tree. In order to provide reliable and resilient multicast services, a common practice is to find two redundant multicast trees from different sources. The redundant multicast tree has to be disjoint with the original multicast tree so that a single edge failure does not disable the multicast service to any destinations [4,6]. In the real life, it is ordinary that some edges are subject to a common risk, and these edges form an SRLG [2,3,9–11]. For example, in communication systems a conduit cut will disable all the optical fibers it contains. In the power distribution network, all power lines located in a geographic area are subject to common risks like nature disaster (e.g., earthquakes, floods, etc.) or terrorism attack. Therefore, an ordinal edge/link disjoint redundant tree is not necessary reliable in these cases, because both paths from two sources to a destination could fail in a single SRLG failure such as a conduit cut or a natural disaster. Finding redundant multicast trees with SRLG-diverse constraints becomes very necessary for reliable multicast service.

In this paper, we present three classes of mix integer programming formulations, edge-based, path-based and tree-based models, for RMR-SRLGD. In particular, we compare the linear relaxations of these formulations for computing lower bounds. For simplicity, we will use the following representations throughout the paper. Let M be a mixed integer programming formulation for RMR-SRLGD. The corresponding linear relaxation is denoted by LM . The value of an optimal solution of the mixed integer formulation is denoted by $\nu(M)$ and the value of an optimal solution of the linear relaxation is denoted by $\nu(LM)$.

The rest of this paper is organized as follows. Section 2 presents the edge-based model. Section 3 presents two alternative path-based models: segregated and aggregated. Section 4 presents a tree-based model. Section 5 presents the computational results of the proposed models. Section 6 draws a conclusion on hierarchy of the LP relaxations of these models.

2 Edge-based model

We shall define the following decision variables for the edge-based model.

y_{ij}^s is a binary variable such that $y_{ij}^s = 1$ if edge (i, j) is included in the multicast tree from source s , and $y_{ij}^s = 0$ otherwise.

x_{ij}^{sd} is a binary variable such that $x_{ij}^{sd} = 1$ if edge (i, j) is used by a path from s to d in the solution, and $x_{ij}^{sd} = 0$ otherwise.

z_b^{sd} is a binary variable such that $z_b^{sd} = 1$ if the path from s to d includes an SRLG $b \in B$, and $z_b^{sd} = 0$ otherwise.

The edge-based model (M_E) is given by

$$(M_E) \quad \min \sum_{s \in S} \sum_{(i,j) \in E} c_{ij} y_{ij}^s \tag{1}$$

$$\text{s.t.} \quad y_{ij}^s - x_{ij}^{sd} \geq 0 \quad \forall (i, j) \in E, \forall s \in S, \forall d \in D, \tag{2}$$

$$\sum_{j|(i,j) \in E} x_{ij}^{sd} - \sum_{j|(j,i) \in E} x_{ij}^{sd} = \sigma_i^{sd} \quad \forall i \in V, \forall s \in S, \forall d \in D, \tag{3}$$

$$z_b^{sd} - x_{ij}^{sd} \geq 0 \quad \forall (i, j) \in E_b, \forall b \in B, \forall s \in S, \forall d \in D, \tag{4}$$

$$\sum_{s \in S} z_b^{sd} \leq 1 \quad \forall b \in B, \forall d \in D, \tag{5}$$

$$x_{ij}^{sd}, y_{ij}^s, z_b^{sd} \in \{0, 1\} \quad \forall (i, j) \in E, \forall b \in B, \forall s \in S, \forall d \in D. \tag{6}$$

The objective function in Eq. 1 minimizes the total cost of two redundant multicast trees. The constraints in Eq. 2 are the logical constraints that ensure an edge must be selected if it is used in a path between a source and a destination in the solution. It notes the aggregated form of Eq. 2 is

$$|D|y_{ij}^s - \sum_{d \in D} x_{ij}^{sd} \geq 0 \quad \forall (i, j) \in E, \forall s \in S. \tag{7}$$

The constraints in Eq. 3 are the flow balance constraints for a path from source s to destination d . In particular, σ_i^{sd} is the net flow capacity at node i . Node i may indicate a source, sink or transshipment node, in a path from source s to destination d . Thus $\sigma_i^{sd} = 1$ if $i = s$, $\sigma_i^{sd} = -1$ if $i = d$, and $\sigma_i^{sd} = 0$ otherwise. The constraints in Eq. 4 are the logical constraints ensuring that an SRLG is selected if any of its edge is included in a path from source s to destination d . The constraints in Eq. 5 ensure that the two paths, each from one of the two sources to every destination, are SRLG-diverse.

3 Path-based models

In this section, we propose two alternative path-based models, segregated and aggregated, for RMR-SRLGD. We prove that the linear relaxation of the segregated model is equivalent to the linear relaxation of the edge-based model. We also prove the linear relaxation of the aggregated model is weaker than that of the edge-based model.

It notes the constraints in Eq. 3 determine the paths from every source to every destination. Therefore, it is intuitive to formulate the problem as a path-based model. In the path-based model, we correspond a decision variable to a path from source $s \in S$ to destination $d \in D$, which arises from the Dantzig-Wolfe decomposition of the edge-based model.

We shall define the following additional notations.

P is a set of all possible paths from any source $s \in S$ to any destination $d \in D$; we also denote P^{sd} as a set of all possible paths from s to d , where $s \in S, d \in D$. We have $P = \bigcup_{s \in S} \bigcup_{d \in D} P^{sd}$; similarly, we define P_{ij}^s as a set of paths from source s using edge (i, j) .

α_{ij}^p is a binary parameter such that $\alpha_{ij}^p = 1$ if path p passes through edge (i, j) , and $\alpha_{ij}^p = 0$ otherwise.

β_b^p is a binary parameter such that $\beta_b^p = 1$ if any edge of path p is a member of SRLG $b \in B$, and $\beta_b^p = 0$ otherwise.

u_p is a binary decision variable such that $u_p = 1$ if path p is selected to form the redundant multicast trees in the solution, and $u_p = 0$ otherwise.

3.1 Segregated path-based model

Given the above additional notations, we can define the segregated path-based model (M_{P1}) as follows.

$$(M_{P1}) \quad \min \sum_{s \in S} \sum_{(i,j) \in E} c_{ij} y_{ij}^s \tag{8}$$

$$\text{s.t.} \quad \sum_{p \in P^{sd}} \alpha_{ij}^p u_p \leq y_{ij}^s \quad \forall (i, j) \in E, \forall d \in D, \forall s \in S, \tag{9}$$

$$\sum_{p \in P^{sd}} u_p = 1 \quad \forall s \in S, d \in D, \tag{10}$$

$$\sum_{s \in S} \sum_{p \in P^{sd}} \beta_b^p u_p \leq 1 \quad \forall b \in B, \forall d \in D, \tag{11}$$

$$u_p, y_{ij}^s \in \{0, 1\} \quad \forall p \in P, \forall (i, j) \in E, \forall s \in S. \tag{12}$$

The objective function in Eq. 8 is the same as in Eq. 1. The constraints in Eq. 9 ensure that an edge must be selected if a path containing that edge is used in the multicast trees. The constraints in Eq. 10 ensure that each source-destination pair is connected by exactly one path. The constraints in Eq. 11 ensure that the two paths connecting the two sources to every destination are SRLG-diverse. We have the following lemma.

Lemma 1 LM_{P1} is equivalent to LM_E . Every feasible solution for LM_{P1} corresponds to a feasible solution for LM_E .

Proof Since every path satisfies the flow balance constraints in Eq. 3, we know

$$\sum_{p \in P^{sd}} \alpha_{ij}^p u_p = x_{ij}^{sd} \quad \forall (i, j) \in E, \forall s \in S, \forall d \in D, \tag{13}$$

$$\sum_{p \in P^{sd}} \beta_b^p u_p = z_b^{sd} \quad \forall s \in S, \forall d \in D. \tag{14}$$

Therefore, we know the constraints in Eq. 2 and the constraints in Eq. 9 are equivalent because of Eq. 13. Similarly, the constraints in Eqs. 4–5 are equivalent to the constraints in Eq. 11 because of Eq. 14. Hence, we conclude the segregated path-based model M_{P1} is equivalent to the edge-based model M_E . \square

3.2 Aggregated path-based model

The aggregated path-based model (M_{P2}) can be formulated as follows.

$$(M_{P2}) \quad \min \sum_{s \in S} \sum_{(i,j) \in E} c_{ij} y_{ij}^s \tag{15}$$

$$\text{s.t.} \quad \sum_{d \in D} \sum_{p \in P^{sd}} \alpha_{ij}^p u_p \leq |D| y_{ij}^s \quad \forall (i, j) \in E, \forall s \in S \tag{16}$$

$$\sum_{p \in P^{sd}} u_p = 1 \quad \forall s \in S, d \in D \tag{17}$$

$$\sum_{s \in S} \sum_{p \in P^{sd}} \beta_b^p u_p \leq 1 \quad \forall b \in B, \forall d \in D \tag{18}$$

$$u_p, y_{ij}^s \in \{0, 1\} \qquad \forall p \in P, \forall (i, j) \in E, \forall s \in S. \tag{19}$$

The formulation in Eqs. 15–19 is the same as formulation MP_1 except the constraints in Eq. 16 are in the aggregated form of the constraints in Eq. 9.

Lemma 2 LM_E is strictly stronger than LM_{P_2} . The worst case ratio $\frac{v(LM_E)}{v(LM_{P_2})}$ is $|D|$.

Proof Here, we need to prove $v(LM_E) \leq v(LM_{P_2})$ for all instances, and there exists some instances such that $v(LM_E) < v(LM_{P_2})$.

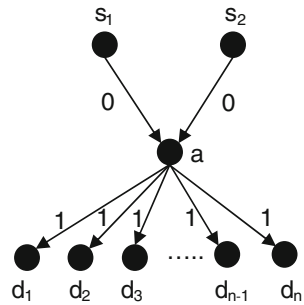
Assume an optimal solution of LM_{P_2} contains a set of paths P'_s from each source s , such that $u_p > 0, \forall p \in P'_s$. It is obvious the edges from each path satisfy the flow balance constraints in Eq. 3. Also, we can see that $z_b^{sd} = \sum_{p \in P^{sd}} \beta_b^p u_p$. Therefore, we know the constraints in Eq. 5 are satisfied. Hence, the edges from the optimal solution of the path-based model LM_{P_2} is a feasible solution for LP relaxation of the edge-based model. Furthermore, we know

$$\begin{aligned} v(LM_{P_2}) &= \sum_{s \in S} \sum_{(i,j) \in E} c_{ij} y_{ij}^s \\ &= \sum_{s \in S} \sum_{(i,j) \in E} \sum_{d \in D} \sum_{p \in P^{sd}} c_{ij} \frac{\alpha_{ij}^p u_p}{|D|} \\ &= \sum_{s \in S} \sum_{(i,j) \in E} \sum_{d \in D} c_{ij} \frac{\sum_{p \in P^{sd}} \alpha_{ij}^p u_p}{|D|} \\ &= \sum_{s \in S} \sum_{(i,j) \in E} \sum_{d \in D} c_{ij} \frac{x_{ij}^{sd}}{|D|} \qquad \text{due to Eq. 13} \\ &= \sum_{s \in S} \sum_{(i,j) \in E} c_{ij} \frac{\sum_{d \in D} x_{ij}^{sd}}{|D|} \\ &\leq \sum_{s \in S} \sum_{(i,j) \in E} c_{ij} y_{ij}^s \qquad \text{due to Eq. 7} \\ &= v(LM_E). \end{aligned}$$

Similarly, we have

$$\begin{aligned} v(LM_{P_2}) &= \sum_{s \in S} \sum_{(i,j) \in E} c_{ij} \frac{\sum_{d \in D} x_{ij}^{sd}}{|D|} \\ &\geq \sum_{s \in S} \sum_{(i,j) \in E} c_{ij} \frac{\max_{d \in D} x_{ij}^{sd}}{|D|} \\ &= \sum_{s \in S} \sum_{(i,j) \in E} c_{ij} \frac{y_{ij}^s}{|D|} \\ &= \frac{1}{|D|} v(LM_E). \end{aligned}$$

Fig. 1 An example of RMR-SRLGD where $v(LM_E) \geq v(LM_{P2})$. Here, $v(LM_E) = 2n > v(LM_{P2}) = 2$



Now, consider an example in Fig. 1. We have two source nodes s_1 and s_2 and a set of destination nodes from d_1 to d_n . We assume that $c_{s_1,a} = c_{s_2,a} = 0$ and $c_{a,d_1} = \dots = c_{a,d_n} = 1$. We also assume each edge is an SRLG by itself. Then it is obvious $v(LM_E) = 2n$ and $v(LM_{P2}) = 2$. Hence, we know $v(LM_E) < v(LM_{P2})$ for some instance. Therefore, we know the edge-based model has stronger LP relaxation than the aggregated path-based model. \square

4 Tree-based model

We also propose a tree-based model in which each decision variable corresponds to a multicast tree from a source to all the destinations. We define the set of additional notations as follows:

T_s is a set of multicast tree connecting source node $s \in S$ to all the destination nodes. T is a superset of T_s , and $T = \bigcup_{s \in S} T_s$.

c_t is the cost of the multicast tree $t \in T$, and $c_t = \sum_{(i,j) \in t} c_{ij}$.

γ'_{bd} is a binary parameter such that $\gamma'_{bd} = 1$ if the path from s to d in a multicast tree t contains SRLG b , and $\gamma'_{bd} = 0$ otherwise. Since a path between any two nodes in a multicast tree is unique, we can explicitly identify the value of γ'_{bd} for any combination of b, d and t .

w_t is a binary decision variable such that $w_t = 1$ if multicast tree t is selected in the solution, and $w_t = 0$ otherwise.

Given the above new notations, we present the tree-based model M_T as following:

$$(M_T) \quad \min \sum_{s \in S} \sum_{t \in T_s} c_t w_t \tag{20}$$

$$\text{s.t.} \quad \sum_{t \in T_s} w_t = 1 \quad \forall s \in S, \tag{21}$$

$$\sum_{s \in S} \sum_{t \in T_s} \gamma'_{bd} w_t \leq 1 \quad \forall b \in B, \forall d \in D, \tag{22}$$

$$w_t \in \{0, 1\} \quad \forall t \in T, \forall (i, j) \in E. \tag{23}$$

The constraints in Eq. 21 ensure that a multicast tree is selected for each source node. The constraints in Eq. 22 satisfy the SRLG-diverse constraints for every group-destination pair.

Lemma 3 LM_T is strictly stronger than LM_E .

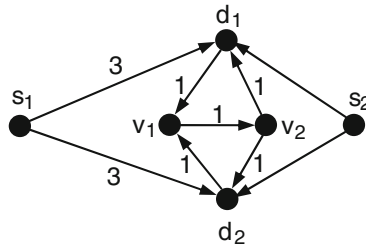


Fig. 2 An example of RMR-SRLGD problem where $v(LM_T) > v(LM_E)$. Two multicast trees $t_{s_1}^1$ and $t_{s_1}^2$ from s_1 and one multicast tree t_{s_2} from s_2 are in the solution. $t_{s_1}^1$ contains edge $s_1 \rightarrow d_1, d_1 \rightarrow v_1, v_1 \rightarrow v_2$, and $v_2 \rightarrow d_2$. $t_{s_1}^2$ contains edges $s_1 \rightarrow d_2, d_2 \rightarrow v_1, v_1 \rightarrow v_2$, and $v_2 \rightarrow d_2$. In the LP solution, $w_{t_{s_1}^1} = w_{t_{s_1}^2} = 0.5$ and $w_{t_{s_2}} = 1 \cdot v(LM_T) = 12 > v(LM_E) = 11.5$

Proof We need to prove $v(LM_T) \geq v(LM_E)$ for all instances, and there exists some instance such that $v(LM_T) > v(LM_E)$.

Assume LM_T contains a set of trees T'_s from each source s , such that $w_t > 0, \forall t \in T'_s$. We can construct a set of paths P_t from each tree $t \in T'_s$. Each path $p \in P_t$ is from source s to a destination $d \in D$. It is obvious that edges from each path satisfy the flow balance constraints in Eq. 3. Also, we can see that $z_b^{sd} = \sum_{t \in T'_s} \gamma_{bd}^t w_t$. Therefore, we know the constraints in Eq. 5 are satisfied. Hence, the edges from the optimal solution to the tree-based model is a feasible solution to LP relaxation of the edge-based model. Furthermore, we know

$$v(LM_T) = \sum_{s \in S} \sum_{t \in T'_s} c_t w_t = \sum_{s \in S} \sum_{t \in T'_s} \sum_{(i,j) \in t} c_{ij} y_{ij}^s \geq \sum_{s \in S} \sum_{(i,j) \in \bigcup_{e \in T'_s} \{e\}} c_{ij} y_{ij}^s = v(LM_E).$$

Now, consider an example in Fig. 2. We have two sources s_1 and s_2 and two destinations d_1 and d_2 . We assume that each edge is an SRLG by itself and the cost is shown in the figure. In LM_E , we have two trees from s_1 , the first tree $t_{s_1}^1$ contains edges $s_1 \rightarrow d_1, d_1 \rightarrow v_1, v_1 \rightarrow v_2$, and $v_2 \rightarrow d_2$. The second tree $t_{s_1}^2$ contains edges $s_1 \rightarrow d_2, d_2 \rightarrow v_1, v_1 \rightarrow v_2$, and $v_2 \rightarrow d_2$. There is a tree from s_2 , which contains edges $s_2 \rightarrow d_1$ and $s_2 \rightarrow d_2$. We know $c_{t_{s_1}^1} = c_{t_{s_1}^2} = c_{t_{s_2}} = 6, w_{t_{s_1}^1} = w_{t_{s_1}^2} = 0.5$ and $w_{t_{s_2}} = 1$. Hence, it is obvious that $v(LM_T) = 12$.

However, in LM_E we have $y_{d_1, d_1} = y_{s_1, d_2} = y_{d_1, v_1} = y_{d_2, v_1} = y_{v_1, v_2} = y_{v_2, d_1} = y_{v_2, d_2} = 0.5$, and $y_{s_2, d_1} = y_{s_2, d_2} = 1$. Therefore, $v(LM_E) = 11.5 < v(LM_T) = 12$. Hence, we know $v(LM_T) \geq v(LM_E)$, and there exists some instance such that $v(LM_T) > v(LM_E)$. \square

5 Computational study

In this section, we discuss the computational study for RMR-SRLGD. We first present the evaluation test instances used throughout the computational study. Then, we detail the computational study of the proposed models. In particular, we compare the LP and IP results of all four models.

5.1 Test instances

In this study, we evaluated the developed formulations by testing them on four test cases. Table 1 presents the characteristics (network topologies) of the four network instances used in

Table 1 Characteristics of test instances

Test instance	# Of nodes	# Of edges	# Of destinations	# Of SRLGs	Ave SRLG size
NET1	21	72	10	22	2.9
NET2	24	86	10	32	2.8
NET3	178	886	33	212	7.5
NET4	178	886	60	212	7.5

this study. NET1 and NET2 refer to the topologies of the Italian and US networks published in [9]. Note that each topology is listed with its name and number of nodes and bi-directional edges. We identify the SRLGs in the network by using the risk relationship among the edges that are identified in [9].

NET3 and NET4 are based on the same operational tier-1 backbone network located across the US from a commercial telecommunication company. Using the information about real fiber spans, we identified SRLGs associated with interfaces, links, and fiber spans as follows. We first associated a unique SRLG with each link, interface, and fiber span that comprise the edge. A SRLG may be used by multiple edges, and likewise, multiple edges may belong to a common SRLG. Then, we removed those SRLGs which are strict subset of other SRLGs. We determined the locations of sources and destinations for NET3 and NET4 as follows. Let us consider NET3 for example. We mapped 40 largest cities in the US as potential destination locations and searched for the nodes that are located geographically closest to those potential endpoints. We identified 33 distinct backbone nodes as destinations for NET3. We also selected the location of two sources of NET3 randomly, one from East Coast and the other one from West Coast. Similarly, the same procedure was performed for NET4.

5.2 Computational experience

All test cases were solved using an Intel Dual Core 2.79 GHz workstation with 1 Gigabytes of memory running Windows XP. Computational times reported in this section were obtained from the desktop's internal timing calculations, which include the time used for preprocessing, perturbation, and postprocessing. All the mathematical modeling and algorithms were implemented in C++. Each LP and MIP problem was solved through a callable CPLEX library version 10.0 with a default setting.

For NET1 and NET2, we solved the LP relaxations of four models presented in the paper by enumerating all possible variables. When the number of the variables are too large to enumerate, we generated at least 500,000 variables. For NET3 and NET4, we used a column generation method discussed in [5] to generate good variables (paths and trees). When solving the MIP formulation of the problem, we stopped the CPLEX procedure if the computational time exceeded 4 hour.

In Table 2, we indicated, for four different models and all test cases, the problem sizes and the computational results. The problem size contains the number of columns and the number of rows in the model. The computational result contains the total computational times, objective values for LP and IP solutions, and the gaps between LP and optimal IP (computed as $\frac{OptimalIP-v(LM)}{OptimalIP}$), and IP solution optimality gap (computed as $\frac{OptimalIP-v(M)}{OptimalIP}$).

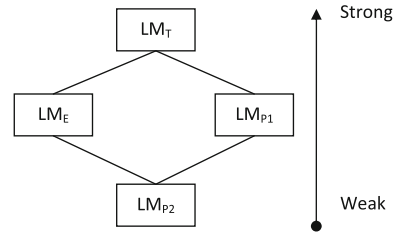
From Table 2, we obtained optimal solutions for NET1 and NET2 test cases in less than 5 minutes of computational time using all the methods. Within these models, M_T provided the best LP-IP solution gap. For NET3, M_E and M_T obtained the optimal IP solution, and LP

Table 2 Comparison between different models

Test case	Model	Problem size		LP solution		IP solution			
		Cols	Rows	Time	Obj	LP gap (%)	Time	Obj	Opt gap (%)
NET1	M_E	2,114	3,780	1	1,375	0.72	2	1,385	0.00
	M_{P1}	13,366	1,680	1	1,375	0.72	5	1,385	0.00
	M_{P2}	13,366	444	1	306	77.91	283	1,385	0.00
	M_T	500,000	222	2	1,385	0.00	17	1,385	0.00
NET2	M_E	2,532	4,320	1	1,955	0.00	2	1,955	0.00
	M_{P1}	13,340	2,060	1	1,955	0.00	25	1,955	0.00
	M_{P2}	13,340	512	1	404	79.34	13	1,955	0.00
	M_T	500,000	322	2	1,955	0.00	15	1,955	0.00
NET3	M_E	67,040	168,564	21	4,421	3.54	1,941	4,583	0.00
	M_{P1}	500,256	65,538	14,400	4,736	6.57	14,400	4,884	6.16
	M_{P2}	500,278	8,834	306	765	83.30	14,400	5,126	11.11
	M_T	668	6,998	3,754	4,577	1.08	4,469	4,583	0.00
NET4	M_E	133,532	331,440	129	6,661	2.06	14,400	6,801	0.00
	M_{P1}	500,592	119,160	14,400	7,235	6.43	14,400	7,238	6.43
	M_{P2}	500,604	14,612	527	871	92.25	14,400	7,880	15.87
	M_T	932	12,722	6,946	6,793	0.12	9,378	6,801	0.00

M_E represents the edge-based model, M_{P1} represents the segregated path-based model, M_{P2} represents the aggregated path-based model, M_T represent the tree-based model

Fig. 3 A hierarchy of linear relaxations of four formulations. M_E represents the edge-based model, M_{P1} represents the segregated path-based model, M_{P2} represents the aggregated path-based model, M_T represent the tree-based model. The models in the upper level provide better LP bounds



gap provided by M_T is only 1/3 of the gap provided by M_E . However, the computational time of M_T is longer than that of M_E , because the pricing subproblem of M_T is time consuming. We did not get the optimal LP and IP solution using the M_{P1} , because the column generate method of M_{P1} converged very slowly. On the other hand, M_{P2} provided an LP relaxation solution with very large LP gap in short time. Both M_{P1} and M_{P2} provided non-optimal integer solutions for NET3 within the time limit. For NET4, M_T provided very tight LP bound and obtained optimal IP solution faster than M_E . Although M_E generated the optimal IP solution within the time limit, CPLEX did not prove the optimality of the solution within the time limit. Both M_{P1} and M_{P2} failed to obtain the optimal IP solution within time limit because of the slow convergence and the poor LP bound.

From the computational results, we can see M_E perform very good for small and mid-sized test cases (NET1-NET3), whereas M_T perform better in very large test cases (NET4). This is because when the test problem is too large for M_E to solve quickly, it is worth to decompose the problem into much smaller subproblems and then use M_T to solve the problem. Finally, it is worth to mention that M_{P2} provided very poor LP bound when the number of destination is large. This is because in LM_{P2} , the aggregated constraints in Eq. 16 are “Big-M” type constraints, and hence the LP-IP gaps provided by LM_{P2} are very large. This observation also corroborates the conclusion of Lemma 2, that is, the worst gap of LM_{P2} could be as large as $\frac{|D|-1}{|D|}$.

6 Conclusion

Figure 3 summarizes the hierarchical relationships of all four mathematical formulations proposed here. The relaxations in the same level are equivalent. A line between two boxes means that the relaxation in the upper box are strictly stronger than the one in the lower box.

It is worthy mentioning that a better LP bound may improve the computational time of an optimal integer solution dramatically. On the other hand, the difficulty of the LP relaxations of the different models could vary a lot. In particular, the number of possible paths increases exponentially with the number of edges in the problem, and the number of possible multicast trees increases exponentially with the number of possible paths. Therefore, it is almost impossible to enumerate all the paths and trees explicitly in the model. We believe it is necessary and important to balance between a good LP bound and the computational time to archive the best performance when dealing with the very large problems.

References

1. Garey, M.R., Johnson, D.S.: Computers and Intractability: A Guide to the Theory of NP-Completeness. W.H. Freeman and Company, San Francisco (1979)

2. Guo, L., Yu, H., Li, L.: A new shared-path protection algorithm under shared risk link group constraints for survivable wdm mesh networks. *Opt. Commun.* **246**, 285–295 (2005)
3. Hu, J.Q.: Diverse routing in mesh optical networks. *IEEE Trans. Commun.* **51**(3), 489–494 (2003)
4. Irava, V.S., Hauser, C.: Survivable low-cost low-delay multicast trees. *Proceedings of Global Telecommunications Conference GLOBECOM '05*, pp. 109–115. (2005)
5. Liang, Z., Chaovallitwongse, W.A., Cha, M., Moon, S., Shaikh, A., Yates, J.: An iptv routing problem with hop constraints. Technical report, Department of Industrial & Systems Engineering, Rutgers, The state University of New Jersey, New Brunswick (2009)
6. Medard, M., Finn, S.G., Barry, R.A.: Redundant trees for preplanned recovery in arbitrary vertex-redundant or edge-redundant graphs. *IEEE/ACM Trans. Netw.* **7**(5), 641–652 (1999)
7. Pardalos, P., Khoury, B.: A heuristic for the steiner problem on graphs. *Comp. Opt. Appl.* **6**, 5–14 (1996)
8. Paul, P., Raghavan, S.V.: Survey of multicast routing algorithms and protocols. *Proceedings of the Fifteenth International Conference on Computer Communication (ICCC 2002)*, pp. 902–926 (2002)
9. Shen, L., Yang, X., Ramanurthy, B.: Shared risk link group (srlg)-diverse path provisioning under hybrid service level agreements in wavelength-routed optical mesh networks. *IEEE/ACM Trans. Netw.* **13**(4), 918–931 (2005)
10. Yuan, S., Jue, J.P.: Dynamic lightpath protection in wdm mesh networks under wavelength-continuity and risk-disjoint constraints. *Comput. Netw.* **48**, 91–112 (2005)
11. Zang, H., Ou, C., Mukherjee, B.: Path-protection routing and wavelength assignment (RWA) in WDM mesh networks under duct-layer constraints. *IEEE/ACM Trans. Netw.* **11**(2), 248–258 (2003)